Journal Pre-proofs

Influence of initial chemical composition and characteristics of pulps on the production and properties of lignocellulosic nanofibers

N.V. Ehman, A.F. Lourenço, B.H. McDonagh, M.E. Vallejos, F.E. Felissia, P.J.T. Ferreira, G. Chinga-Carrasco, M.C. Area

PII: S0141-8130(19)34812-3
DOI: https://doi.org/10.1016/j.ijbiomac.2019.10.165
Reference: BIOMAC 13666

To appear in: *International Journal of Biological Macromolecules*

Received Date: 27 June 2019
Revised Date: 11 October 2019
Accepted Date: 18 October 2019

Please cite this article as: N.V. Ehman, A.F. Lourenço, B.H. McDonagh, M.E. Vallejos, F.E. Felissia, P.J.T. Ferreira, G. Chinga-Carrasco, M.C. Area, Influence of initial chemical composition and characteristics of pulps on the production and properties of lignocellulosic nanofibers, *International Journal of Biological Macromolecules* (2019), doi: https://doi.org/10.1016/j.ijbiomac.2019.10.165

Influence of initial chemical composition and characteristics of pulps on the production and properties of lignocellulosic nanofibers

Ehman N.V.[a*], Lourenço A.F.[b], McDonagh B.H.[c], Vallejos, M.E.[a], Felissia F.E.[a], Ferreira P.J.T.[b], Chinga-Carrasco G.[c], Area M.C.[a]

a) IMAM, UNaM, CONICET, FCEQYN, Programa de Celulosa y Papel (PROCYP), Misiones, Argentina, Félix de Azara 1552, Posadas, Argentina

b) CIEPQPF, Department of Chemical Engineering, University of Coimbra, Pólo II, R. Silvio Lima 3030-790, Coimbra, Portugal

c) RISE PFI, Høgskoleringen 6b, Trondheim, Norway

**Corresponding author:* 1552 Félix de Azara St. ZIP Code 3300, Posadas, Misiones, Argentina. Phone: +54-376-154681157, nanciehman@gmail.com

ABSTRACT

This work aimed to study the influence of the initial chemical composition (glucans, lignin, xylan, and mannans), intrinsic viscosity, and carboxylate groups of pulps on the production process and final properties of lignocellulosic nanofibers (LCNF). Pulps of pine sawdust, eucalyptus sawdust, and sugarcane bagasse subjected to conventional pulping and highly oxidized processes were the starting materials. The LCNF were obtained by TEMPO mediated oxidation and mechanical fibrillation with a colloidal grinder. The nanofibrillation degree, chemical charge content, rheology, laser profilometry, cristallinity and atomic force microscopy were used to characterize the LCNF. The carboxylate groups, hemicelluloses and lignin of the initial pulps were important factors that affected the production process of LCNF. The results revealed that intrinsic viscosity and carboxylate groups of the initial pulps affected LCNF production process, whereas lignin and hemicelluloses influenced the viscosity of LCNF aqueous suspensions, the roughness of LCNF films, and the carboxylate groups content of LCNF.

KEYWORDS: lignocellulosic nanofibers; pine and eucalyptus sawdust; sugarcane bagasse

1. Introduction

The valorization of residual biomass has gained interest in recent years since taking advantage of lignocellulosic wastes allows the reduction of raw material costs and environmental impact. Intermediate and final products (chemicals, fuels, and solvents) are obtained from the principal chemical components of lignocellulosic materials [1]. The fractionation process is selected according to the product to be obtained. The main process options for the selective fractionation of hemicelluloses from lignocellulosic materials include the use of acids, water, steam, organic solvents, and alkaline agents [2]. The hemicelluloses fraction is a precursor of high value-added products such as ethanol, furans, glycerol and derivatives, lactic acid, succinic and levulinic acid, sorbitol, and xylitol [3]. Different fractionation processes can be applied to separate lignin from biomass [4]. Dissolved lignin is also a source of added-value products, like phenols adhesives, biodegradable foams, vanillin, lignin-based polymer materials, active carbon, and carbon fibers/nanofibers, among others [5–7].

Cellulose nanoscale materials from renewable resources such as cellulose nanocrystals (CNC), cellulose nanofibers or lignocellulosic nanofibers (CNF or LCNF), and bacterial cellulose (BC) [8] have opened new perspectives for the development of sustainable and innovative products. CNF or LCNF have demonstrated a good potential to different applications [9], like packaging [10,11], printed electronics [12], 3D printing [13,14], biocomposites [15], and functionalized aerogels for specific uses [16,17].

LCNF are aggregates of cellulose chains that form elongated cylindrical structures with diameters and lengths in the order of nanometers (nm) and micrometers, respectively. They are obtained from cellulosic pulps that contain different amounts of lignin and hemicelluloses. Gel-like suspensions of LCNF are generally prepared at 1% consistency. The evaluation of LCNF properties is of relative importance to determine whether a given gel-like suspension achieves the specifications required for final applications. Commonly measured properties are the degree of fibrillation [18,19] amount of nanofibers [20–22], morphology [23], rheology [24,25], crystallinity [26], specific superficial area [27] and chemical bonds [27–29]. In recent years, the different factors that influence the final properties of LCNF have been studied, including the type of raw material, production process, and content of chemical components in pulps [27–31]. Biomass waste represents a

massive and renewable resource for the production of LCNF. The raw materials studied by various authors include residues of the primary industrialization of wood and straw wastes, being these last ones the more important in quantity. Tarrés *et al*. (2017) used a hybrid wheat straw named triticale (*X Triticosecale Wittmack*) to produce LCNF and evaluated its final properties. Espinosa *et al*. (2015) used wheat straw to produce LCNF and then applied the obtained gel-like suspensions in semi-chemical pulps to evaluate the improvement of the physical-mechanical properties of papers. Some authors have used sugarcane bagasse as raw material for CNF for various applications; *e.g*., reinforcement in paper [32] [33]; inks for 3D printing [14] and as a humidity sensing substrate for packaging and biomedical applications [34]. Regarding wood residues, Ehman *et al*. (2016) studied the production of LCNF from pine sawdust, a waste of the primary industrialization of wood and Vallejos *et al*. (2016) evaluated the influence of LCNF obtained from eucalyptus sawdust as reinforcement in papers from eucalyptus pulp. Sánchez *et al.* (2016) used wheat straw pulps from soda, kraft, and organosolv pulping processes to obtain LCNF combining chemical and mechanic processes [35].

The production process to obtain CNF or LCNF from biomass includes a stage where the raw material is pulped and, in some cases, a sequence for cellulose purification is added and a second stage where a mechanical treatment or chemical/mechanical treatment is performed. 2,2,6,6-tetramethylpiperidine-1-oxyl (TEMPO) reagent catalyzed oxidation followed by mechanical fibrillation is one of the most used mechanisms to produce CNF and LCNF. The oxidation developed by Saito and Isogai (2004) consists of treating the pulp at 1% consistency using NaBr, NaClO, and TEMPO reagent at pH 10. The treatment is carried out to partially separate the nanofibers and reduce energy consumption during the subsequent mechanical stage. Finally, mechanical stress is applied to the previously oxidized fibers to release the nanofibers. The mechanical fibrillation can be performed using high-pressure homogenizers [37], microfluidizers [38], microgrinding [39], or high-speed blenders [40].

When studying of the effect of bleaching and refining of pulps on the final properties of LCNF, the effect of bleaching on the nanofibrillation yield, cationic demand, and transmittance resulted higher than that of refining [41]. The chemical composition of the

raw material strongly affects some process variables and the quality of the LCNF and the CNF, as stated by several authors. Studies include the effect of lignin [31,42], and xylans [43], but there are still no systematical studies about all the influence of the chemical components on the CNF characteristics.

This study aimed to highlight the key role of the chemical composition, intrinsic viscosity, and carboxylate content of the pulp on LCNF production process and their final properties. Pulps derived from different raw materials and chemical treatments were chemically characterized and subjected to a TEMPO mediated oxidation stage, followed by mechanical fibrillation in a colloidal grinder. The influence of the raw material, the use or not of a conventional pulping or highly oxidized treatments and the variation of the TEMPO load in the production process and final properties of the LCNF were evaluated. These results are important for the optimization of the treatment of raw materials when integrated into lignocellulosic biorefinery schemes.

2. Material and Methods

2.1 Materials

Seven different pulps were selected for this work, based on pine sawdust, eucalyptus sawdust, and sugarcane bagasse (Table 1). A commercial ECF bleached Kraft pulp from pine chips was used as a reference.

For the A pulp, the eucalyptus sawdust was collected from a local sawmill-carpentry and it was subjected to soda pulping. The pulping conditions were: 60 min at 170 ºC with 22% NaOH on oven-dry wood (odw), with a liquid/sawdust ratio of 6/1. The pulp was further delignified by total chlorine-free (TCF) sequence. The conditions of the first oxygen stage were: 3% NaOH over dry pulp (odp) and 0.1% $MgSO_4$ odp at 10% of consistency, 100°C for 60 min, and an oxygen pressure of 6 kg/cm^2. The conditions of the second oxygen stage were: 3% NaOH odp, 0.2% $MgSO_4$ odp, 0.1% of a chelating agent odp, 1% H_2O_2 odp, 10% of consistency, 6 kg/cm^2 of O_2 pressure, at 100°C for 60 min [44].

B and C pulps were commercial pulps. The B pulp was a sugarcane bagasse bleached pulp obtained by a Soda/Anthraquinone (Soda/AQ) treatment with oxygen stage, and the C pulp was an elementary chlorine-free (ECF) bleached kraft pulp from pine chips.

The D pulp was pine sawdust bleached pulp obtained by a Soda/Ethanol (Soda/Et) treatment and TCF bleaching. The pulping conditions were: 35/65 %v/v (Et/H_2O), 19% NaOH odp at 170°C [30,45].

The E pulp was an unbleached pine sawdust pulp obtained by Soda/Et pulp using 35/65 %v/v (Et/H_2O), 19% NaOH odp at 170°C [45].

The F pulp was obtained using a Soda/Oxygen treatment at 150°C, 4 kg/cm^2 O_2 and 80 g L^{-1}, and the G pulp was obtained using a Soda/Oxygen treatment at 160°C, 4 kg/cm_2, 80 g L^{-1} NaOH, 2.2 % Cu odp, and 0.2% Fe odp.

2.2 Methods

2.2.1 Pulp characterization

Acid-insoluble lignin (Klason lignin) and structural carbohydrates were determined according to the NREL/TP-510-42618 procedure "Determination of Structural Carbohydrates and Lignin in Biomass" [46]. A sample of 1 g (odp) of pulp was treated with 72% H_2SO_4 at 30°C for 1 h. Then, the acid was diluted at 4% concentration with deionized water and autoclaved at 121°C for 1 h. The solution was cooled to room temperature, filtered, and the insoluble residue was washed, oven-dried, and finally, lignin insoluble content was determined. Carbohydrates were analyzed by high-performance liquid chromatography using a SHODEX SP810 column connected in series to a BIORAD deionizing pre-column. The chromatographic conditions used were: water as eluent, the flow rate of 0.6 mL/min, 85°C, and a refractive index detector.

The determination of intrinsic viscosity was carried out according to standard ISO 5351/1 *"Pulps-Determination of limiting viscosity number in cupri-ethylenediamine (CED) solution"*, and carboxylate groups of initial pulps through conductimetric titration. Both methods are described in item 2.2.3.

2.2.2 LCNF Preparation

Pulps were subjected to TEMPO mediated oxidation accordingly to [36]: the pulps were suspended in water containing TEMPO (0.24 g) and NaBr (1.5 g) at 1% consistency (1500 mL). When the catalyst was completely dissolved, TEMPO mediated oxidation was started by adding NaClO 10 mmol odp dropwise under continuous stirring and at room temperature. During the reaction time, 0.5 M NaOH was added to maintain the pH at 10 until no decrease in pH was observed. TEMPO mediated oxidized pulps were then washed using distilled water. The TEMPO mediated oxidized pulps at 1.3% consistencies were passed through a colloidal grinder to break completely the fibril bundles until the point when the recirculation of the suspension in the equipment stopped because of the gelification of the material. The mechanism of operation of the colloid grinder involves the recirculation of the NFC suspension. Initially, the sample recirculates easily due to its low viscosity, as the NFCs are released, the viscosity increases reaching a point where recirculation is interrupted. A gel-like dispersion was obtained for all samples.

2.2.3 LCNF Characterization

The nanofibrillation yield was determined for LCNF2, LCNF3, LCNF4, LCNF5, LCNF6, and LCNF7 by centrifuging a 0.2 wt.% of suspension at 9000 rpm for 30 min [23] (8965 g) to separate the nanofibrillated fraction (contained in the supernatant) from the non-fibrillated and partially fibrillated ones, which are retained in the sediment fraction. This last was recovered, and oven-dried at 90 °C until constant weight. The yield of nanofibrillation was then calculated from the next equation:

$$Nanofibrillation\ Yield\ (\%) = \left[1 - \frac{Dry\ precipitated\ weight}{Initial\ dry\ weight}\right]$$

Transmittance measurements were accomplished on 0.1 wt.% solid content LCNF suspensions at 800 nm with a UV–Vis Shimadzu spectrophotometer, using distilled water as reference.

Turbidity was measured on 0.1 % solid content LCNF suspensions after stirring for 60 min. A HACH Model 2100AN laboratory turbidimeter was used, which measures turbidity in a range from 0 to 10,000 NTU (Nephelometric Turbidity Units).

The carboxylate content (CC) of the samples was determined by conductometric titration using 0.25 g of dry sample in 250 mL NaCl at 0.001 M. The suspension was stirred at 500 rpm during 60 min and then the pH of the suspension was adjusted at 3.0 with 0.1 M HCl. The suspension at pH 3.0 was titrated with 0.1 N NaOH by adding 0.25 mL aliquots. The analysis was carried out in an N_2 atmosphere and the conductivity was monitored with a conductimeter HORIBA D-24. The values were obtained from the conductivity curve according to Equation 1 [27]:

Equation 1. Carboxylate groups (CC) in µmol per gram

$$CC\ (\mu mol\ odp) = \frac{(V_2 - V_1)}{m} * 0.1\ N\ NaOH * 1000$$

Where V_2-V_1 is the volume of NaOH added to neutralize the carboxylate groups and m is the mass of LCNF on dry base (g). The results indicate the average of –COOH groups in µmol per gram of LCNF.

Cationic demand (CD) was measured by colorimetric titration adapting the methodology described by Mocchiutti *et al*. [47]. The diluted suspension at 0.04 wt.% was stirred for 60 min at 500 rpm. 10 mL of sample was taken, mixed with 25 mL of 0.001N polydimethyldiallylammonium chloride (polyDADMAC) and stirred for 5 min at 500 rpm. The sample was centrifuged for 10 min at 3000 rpm. 10 mL of supernatant was taken after centrifugation, a few drops of OTB indicator were added and absorbance was measured using a Shimadzu UV-1800 UV-Vis spectrophotometer. Titration was started using potassium polyvinyl sulfate (PVSK) as the negative titrant polymer and for each milliliter added absorbance was measured.

The rheological properties of LCNF dispersions were measured at 25 ±1° C by a Brookfield Rotational Viscometer model DV1 using a vane-type spindle at 0.6 rpm rotation speeds. 100 mL of aqueous dispersions at 0.5% consistency were prepared and then stirred

for 60 min at 500 rpm to reach a homogeneous system. The torque during the measurement was kept between 10% and 50%.

The ξ -potential determination was performed on the supernatant obtained after centrifugation at 9000 rpm for 30 min using a 0.2% consistency suspension in a Malvern Zetasizer Nano ZS (range from 0.6 nanometers to 6 micrometers).

Films of 20 g/m^2 of LCNF1, LCNF3, LCNF5, LCNF6, and LCNF7 were prepared for laser profilometry analysis. The films were prepared from 0.5% consistency suspensions (with prior agitation during 60 min). Suspensions were air-dried in Petri dishes.

The films were mounted on microscopy slides and covered with a layer of gold. Ten laser profilometry images were acquired from the top side of the films. The size of the images was 1 x 1 mm and the resolution 1 μm/pixel. The images were processed with the SurfCharJ plugin for quantification of surface roughness (root-mean-square). For details see (Chinga-Carrasco *et al*., 2014). 1 cm x 1cm of each film was mounted with double-sided tape onto a microscope glass slide. Three AFM images were collected for each film using an AFM Dimension Icon (Bruker) with software Nanoscope 9.4 and ScanAsyst Air set-up. Images were acquired with SA air tips (Silicon tip on nitride lever, f_0=70kHz) with a spring constant of 0.4 N/m. Image size was 2 μm x 2 μm with 1024 samples per line, scan rate 0.998 Hz and an aspect ratio equal to 1. NanoScope Analysis 1.9 software was used to generate images.

The cristallinity of LCNF were measured using PANalytical Empyrean equipment with a monochromatic source CuKα1 over an angular range of 10-80°. Cristallinity index (CI) were calculated using Segal *et al*. method [49].

Statistical analyses were performed using the Statgraphics software. Correlation, Regression, Principal components, and ANOVA tests were applied at a significance level $p < 0.05$. R^2, r, and p values are informed between parentheses.

3. Results and Discussion

The chemical composition and values of intrinsic viscosity and carboxylate groups for the initial pulps are shown in Table 2.

The content of hemicelluloses ranged from 11.7% to 28.4%. In the eucalyptus sawdust pulp (pulp A), the content of hemicelluloses consists exclusively of xylans, whereas in sugarcane bagasse (pulp B) xylans are the main components of the hemicelluloses but other sugars are present in a much smaller proportion. The hemicelluloses in pine pulps (C to G pulps) are composed mainly of xylans and mannans. In the samples subjected to the Soda/Oxygen treatment (F/G pulps), the content of xylans was low, but mannans content remained high.

During the Soda/Oxygen treatment, the generation of oxygen radicals causes a major attack on carbohydrates, the radicals as superoxides and hydroperoxide anions are not selective. Peeling reactions in an alkaline medium in the presence of oxygen affect xylans more than cellulose and glucomannans, differing respect to a peeling without oxygen, where cellulose is more affected than glucomannans [50]. Also, according to intrinsic viscosities, a high degradation of carbohydrates was observed in the samples that were submitted to highly oxidized respect to conventional treatments.

Carboxylates content in initial pulps varied in the range from 15.3 to 208.7 (μmol/g), the highest value of carboxylates content was for the soda/oxygen pulp without catalyzers (F pulp), whilst the lowest value was for the bleached kraft pulp. The high values obtained in some of the samples are due to dissolved colloidal substances that interfere with the conductimetric titration [32], for example in pulp F, where there is an initial insoluble lignin content of 14.5%. Soluble lignin in the samples was negligible because of the numerous stages of treatment. Also, in bleached pulps, the soluble lignin quantification is highly interfered by degradation products as furfural and HMF.

Results of LCNF characterization are shown in Table 3.

3.1 TEMPO mediated oxidation

The endpoint of the TEMPO mediated oxidation is reached when the pH stabilizes because there are no new carboxylate groups that can decrease the pH. The raw material showed a significant influence on the TEMPO mediated oxidation time (p-value =0.00).

The highest value of TEMPO mediated oxidation time was observed for the eucalyptus sawdust pulp. Also, significant differences were found among the conventional and highly

oxidized pulps (*p*-value =0.02). As for the pine pulps, the higher values for the TEMPO mediated oxidation time were obtained in the samples from conventional treatments (C and E pulps). During the TEMPO mediated oxidation there is a continuous generation of carboxylate groups. The highest value of CC was obtained for the bleached kraft pulp (LCNF3). Lower CC values were obtained for samples from pine sawdust. In the case of the LCNF from eucalyptus and bagasse pulps, the obtained values were high despite their preliminary oxidation. The highest values of carboxylate groups were reached by the LCNF from conventional pulps (p-value=0.04).

3.2 Mechanical fibrillation

The mechanical fibrillation stage of the samples after TEMPO mediated oxidation was performed using a colloidal grinder. The nanofibrillation yield varied from 55.1% for LCNF6 to 63.0% for LCNF4 (Table 3). The yields were lower than those obtained using the high-pressure homogenizer (HPH). In previous work, the nanofibrillation yield for LCNF from pine sawdust (with Soda/AQ-O-Z treatment) pulp with TEMPO-mediated oxidation in similar conditions and HPH, was 89.7% [28]. Balea *et al.*[51] obtained similar yields for a refined corn pulp using the same TEMPO-mediated oxidation conditions and HPH (less than 60.0%) and higher values for a bleached corn pulp and rape pulps (higher than 90.0%). Sánchez *et al.* [35] found higher values of fibrillation yield for a wheat straw pulp with the same xylan content using 5 mmols of NaClO in the TEMPO-mediated oxidation and HPH.

The determination of the nanofibrillation yield by centrifugation was not possible in all samples, but a positive correlation (r=+0.95) was found between this property and transmittance values. Since this shows that transmittance is a good indirect method to measure nanofibrillation yield, it was included in Table 3. The transmittances obtained from different pulps using 10 mmol of NaClO odp during TEMPO-mediated oxidation and mechanical fibrillations with different equipment are shown in Figure 1. LCNF from Soda/Ethanol and TCF sequence (D pulp) was also mechanical fibrillated using a high-speed blender (HSB) for 18 min.

The stability of some dispersions of LCNF was evaluated by determining the ξ-potential. Values were higher than -30 mV rendering all the evaluated dispersions stable. Results were similar to those obtained by Gamelas *et al*. (2015) for CNF produced using TEMPO mediated oxidation and mechanical fibrillation.

3.3 LCNF Morphology

LCNF have a complex morphology with various structural components, from residual fibers (micrometer/millimeter-scale) to nanofibers (< 100 nm). It is important to describe the various scales of the LCNF to provide an objective assessment of the materials.

The samples evaluated showed diameters of less than 12 nanometers. The sample Soda/Ethanol (LCNF5) presented the lowest diameter value of the LCNF (8.1 nm) whilst the highest value was for the sample from eucalyptus sawdust pulp of eucalyptus (11.9 nm).

AFM images indicated differences between the samples. A homogenous distribution was observed in LCNF from lignin-free pulps (LCNF1 and LCNF3), however, those LCNF samples from pulps with higher initial content of lignin (LCNF5, 6 and 7) presented a more heterogeneous surface.

Globular particles of nanometric sizes are observed in samples from pulps with lignin. This could be lignin that was dissolved with sodium hypochlorite during TEMPO-mediated oxidation stage, not eliminated during the washing step.

Therefore, laser profilometry was applied (Figure 2) to characterize the surface morphology affected by residual fibers. The more residual fibers LCNF dispersion contains, the rougher is the surface of the corresponding films (Chinga-Carrasco *et al*., 2014).

The roughness of the LCNF films varied between 0.38 μm and 2.45 μm. The highest value was for the sample with the highest lignin content (LCNF6) and the lowest value was for the sample from the eucalyptus sawdust pulp. There was a great difference between the viscosities at 0.5% consistency (Table 3) in pulps with conventional or highly oxidized treatments. Moreover, in the case of pine samples prepared with conventional pulping, there are differences between using chips or sawdust. One of the most important factors affecting the rheology of nanocellulose-containing aqueous dispersions is the morphology

(size and shape) of the nanofiber [52], which includes nanofibers length, diameter, and degree of fibrillation. The effect of length on viscosity values was evaluated previously by [53] who found a linear relationship between viscosity values and the length of the nanofiber. According to the AFM analysis, there was no apparent difference between the diameters of the samples so it is possible to assume that there are differences in their lengths.

3.4 Relationships between variables

3.4.1 TEMPO- mediated oxidation time

A negative correlation was found between TEMPO- mediated oxidation time and insoluble lignin content of pulps (r=-0.94). Higher insoluble lignin content causes a decrease in the time of TEMPO mediated oxidation time for sugarcane bagasse and pine pulps. Lignin could react with the ClO^- in alkaline conditions consuming all the primary oxidant and causing a quick ending of the reaction with a minor amount reacting with the OH groups of the C6 of the cellulose. The LCNF3 sample followed by the LCNF1 sample, both practically free of lignin, showed the highest CC values, whilst the samples with the highest initial lignin content in pulp showed lower CC values. The increase in time for pulps with lower amounts of lignin is due to an increase in the amount of oxidized OH groups, which facilitates the fibrillation during the mechanical stage. Similar behavior was previously observed in the values of transmittance concerning the initial lignin content, therefore, it is expected that the transmittance values increase with increased oxidation time and that turbidity values will decrease as the concentration of the primary oxidant decreases. A negative correlation (r=-0.91) was found between the carboxylate content of the initial pulps and the TEMPO-mediated oxidation time. That is, the increase in carboxylate groups (R^2=0.81) of initial pulps decreases the time required for oxidation (Figure 3).

3.4.2 Mechanical fibrillation time

Hemicelluloses content correlated negatively (r=-0.90) with fibrillation time of the pine samples. The higher the content of hemicelluloses, the shorter the time required in the fibrillation equipment (R2=0.81) (Figure 4.a). This is an important conclusion if the objective is to include the LCNF in a biorefinery scheme.

For all samples, a negative correlation (r=-0.81) was found between hemicelluloses of pine pulps and fibrillation time of LCNF production (Figure 4 a). A negative correlation (r=-0.90) was found between the carboxylate groups of LCNF and the mechanical fibrillation time. This coincides with previous studies carried out with pine sawdust [28], eucalyptus pulp [54] and wheat straw [27]. The correlation can be due to the fiber charge that strongly influences the swelling of wet fibers, fiber flexibility, fiber–fiber bonding, and refinability. The more oxidized the samples, the lower the time required for mechanical fibrillation (R^2=0.82) (Figure 4.b). Samples with high lignin content can be seen to depart slightly from the linear behavior, which can be an effect of lignin ability to consume the primary oxidant and thus reduce the CC content in the obtained LCNF.

3.4.3 Relationships involving fibrillation degree

The nanofibrillation yield is an indicative measure of the degree of fibrillation of the sample. That is, an increase in the nanofibrillation yield implies that the sample is more nanofibrillated. Another variable frequently used as indicative of the degree of fibrillation is transmittance, scanner transmittance, turbidity, and fibers fraction determination [19].

In Figure 5.a is showed a positive correlation between nanofibrillation yield and transmittance, and in Figure 5.b a negative correlation between the yield of nanofibrillation and turbidity (r=-0.90). However, there is a positive correlation (r=+0.99) between nanofibrillation yield and viscosity only for conventional pulps (Figure 5.a).

The relationships between the fibrillation degree and turbidity, transmittance, and viscosity can be used only for the colloid grinder because the fibrillation produced by this equipment is less than that of the HPH. However, several studies have shown that the degree of fibrillation correlates with transmittance [27,32,55] and turbidity [19].

3.4.3 Apparent viscosity of LCNF aqueous dispersions

The influence of the initial intrinsic viscosity in CED solution of pulps on the final LCNF viscosities was observed for all pulps except the eucalyptus one. Conventional pulps of pine and sugarcane bagasse that have a higher initial value of intrinsic viscosity generate LCNF with high viscosities, whereas pine pulps with low viscosities reach LCNF with lower

apparent viscosities (Figure 6). Pine sample LCNF3 and sugarcane bagasse sample LCNF2 showed the highest viscosities whereas eucalyptus sawdust sample LCNF1 showed the lowest.

The latter behaved in a very different way than the other samples and the morphology analysis by profilometry showed clear differences in roughness (Figure 2) verified by the ANOVA analysis, which revealed significant differences between raw materials (*p*-value=0.02) and between pulping treatments (*p*-value=0.00).

3.4.4 Carboxylate groups content of LCNF

Hemicelluloses content of initial pulps correlated positively (r=+0.89) with carboxylate groups content of LCNF of the pine samples. The higher the content of hemicelluloses, the higher the carboxylate content of LCNF, considering the range of hemicelluloses between 11.7 and 18.9% odp (R^2=0.80) (Figure 7).

Good correlations between lignin, xylans, mannans, and surface roughness by laser profilometry were found when analyzing five samples (+0.83, -0.81, and +0.68, respectively). Samples with high amounts of lignin yielded rougher surfaces, indicating a larger occurrence of residual fibers and a lower nanofibrillation degree. On the contrary, higher xylans amounts yield a smoother surface indicating a minor fraction of residual fibers. Xylans promote the content of carboxylate groups as demonstrated in this study: the more oxidized the samples the easier the nanofibrillation during the homogenization process. On the other side, high mannans content increases the surface roughness of the corresponding films, indicating a higher fraction of residual fibers and a lower fraction of nanofibrils. Mannans amount impacts negatively on the generation of carboxylate groups, and lower fibrillation is thus expected.

Principal component analysis (PCA) is a multivariate analysis technique of data reduction, which transforms original measured data into a small number of new uncorrelated variables called principal components (PCs), which explain the majority of the variance observed. In this case, two components were identified producing 90% of the variation.

C1 = -0.3 pulp carboxylic groups -0.3 lignin -0.3 turbidity -0.3 z potential +0.2 hemicelluloses + 0.3 oxidation time + 0.3 centrifuge yield +0.3 transmittance +0.3 viscosity +0.3 LCNF carboxylic groups +0.3 crystallinity

C2= -0.4 intrinsic viscosity -0.3 hemicelluloses - 0.2 crystallinity -0.3 cationic demand + 0.4 glucans +0.3 fibrillation time + 0.3 centrifuge yield + 0.4 D by AFM

All the variables involved in C1 have the same relative weight, although some of them influence the component in a positive and others in a negative way. Knowing the individual effect of each of these variables on the nanofibrillation process, it can be concluded that C1 merges the strongly correlated parameters which represent a highly fibrillated LCNF.

On the contrary, in C2, intrinsic viscosity, glucans, and diameter are the factors of greatest weight, while crystallinity has less influence. In this case, it is clear - by the level of influence and the sign - that C2 represents a greater difficulty of fibrillation.

4. Conclusions

The influence of initial chemical composition, intrinsic viscosity and carboxylate groups of cellulosic pulps obtained by conventional and highly oxidized treatments on the production process and final properties of LCNF were evaluated.

The highest value of TEMPO-mediated oxidation time was for eucalyptus sawdust pulp. In the case of pine pulps, higher times were required for pulps with conventional pulping. A strong relationship was found between the oxidation time and insoluble lignin content of pulps. The shortest fibrillation time was reached for the bleached kraft pine pulp. The higher the content of hemicelluloses, the shorter the time required in the fibrillation equipment. Even if the achieved nanofibrillation yield were higher than 50%, they were lower than those obtained by high pressure homogenization. Very strong relationships were found between nanofibrillation yield and viscosity at 0.5% consistency, transmittance, and turbidity. Conventional pulps of pine and sugarcane bagasse that have a higher initial value of intrinsic viscosity generate LCNF with higher viscosities.

Hemicelluloses content of initial pulps correlated positively with carboxylates groups of LCNF of the pine samples. Since it is known that carboxylate content directly affects

fibrillation performance, a high hemicelluloses content in pulps will cause higher yields of nanofibers in the suspensions. The roughness of the LCNF films varied between 0.38 μm and 2.45 μm. Good correlations between lignin, xylans, mannans, and surface roughness determined by laser profilometry were found. These results are consistent with the above described, so roughness can be considered a reflection of fibrillation performance.

All the samples showed diameters of less than 12 nanometers.

According to the principal component analysis (PCA), two components were identified producing 90% of the variation, the first representing the highly fibrillated LCNF and the second representing higher difficulty of fibrillation.

5. Acknowledgments

The authors acknowledge the National Scientific and Technical Research Council (CONICET, Argentina), the National University of Misiones (Argentina), the University of Coimbra (Portugal), FCT for SFRH/BDE/108095/2015 grant, CYTED-NANOCELIA network, and the ValBio-3D project Grant ELAC2015/T03-0715 (Ministry of Science, Technology and Innovation Production of Argentina, and Research Council of Norway, Grant no. 271054).

6. References

[1] M.C. Area, M.E. Vallejos, Biorrefinerías a partir de residuos lignocelulósicos, Editorial Academica Española, Saarbrücken, 2012.

[2] F.M. Gírio, C. Fonseca, F. Carvalheiro, L.C. Duarte, S. Marques, Hemicelluloses for fuel ethanol: A review, Bioresour. Technol. 101 (2010) 4775–4800. doi:10.1016/j.biortech.2010.01.088.

[3] J.L. Wertz, M. Deleu, S. Copée, A. Richel, Hemicellulose and lignin in biorrefineries, Taylor & Francis Group, Boca Raton, 2018.

[4] M.N. Collins, F. Tanas, A. Mcloughlin, A. Stró, M. Culebras, C. Teac, International Journal of Biological Macromolecules Valorization of lignin in polymer and composite systems for

advanced engineering applications – A review, 131 (2019) 828–849. doi:10.1016/j.ijbiomac.2019.03.069.

[5] C. Flores, J. Dobado, J. Isac-García, F. Martín-Martinez, Lignin an lignans as renewable raw materials, Wiley, Chichester, 2015.

[6] N. Dalton, R.P. Lynch, M.N. Collins, M. Culebras, Thermoelectric properties of electrospun carbon nano fi bres derived from lignin, Int. J. Biol. Macromol. 121 (2019) 472–479. doi:10.1016/j.ijbiomac.2018.10.051.

[7] M. Culebras, M. Sanchis, A. Beaucamp, M. Carsí, B. Kandola, R. Horrocks, G. Panzetti, C. Birkinshaw, M.N. Collins, Understanding the thermal and dielectric response of organosolv and modified kraft lignin as a carbon fibre precursor, Green Chem. 20 (2018) 4461–4472. doi:10.1039/c8gc01577e.

[8] A. Blanco, C. Monte, C. Campano, A. Balea, N. Merayo, C. Negro, Nanocellulose for Industrial Use: Cellulose Nanofibers (CNF), Cellulose Nanocrystals (CNC), and Bacterial Cellulose (BC), in: C.M. Hussain (Ed.), Handb. Nanomater. Ind. Appl. Micro Nanotechnologies, 2018: pp. 74–126. doi:https://doi.org/10.1016/B978-0-12-813351-4.00005-5.

[9] C.J. Chirayil, L. Mathew, S. Thomas, Review of recent research in nanocellulose preparation from different lignocellulosic fibers, Rev. Adv. Mater. Sci. 37 (2014) 20–28.

[10] H. Azeredo, M. Rosa, L. Henrique, C. Mattoso, Nanocellulose in bio-based food packaging applications, Ind. Crop. Prod. 97 (2017) 664–671. doi:10.1016/j.indcrop.2016.03.013.

[11] B.F. Li, E. Mascheroni, L. Piergiovanni, The Potential of NanoCellulose in the Packaging Field : A Review, (2015). doi:10.1002/pts.

[12] F. Hoeng, A. Denneulin, J. Bras, Use of nanocellulose in rinted electronics: A review, Nanoscale. 8 (2016) 13131–13154. doi:10.1039/C6NR03054H.

[13] T. Syrový, S. Maronová, P. Kuberský, N. Ehman, M. Vallejos, S. Pretl, F. Felissia, M.C. Area, G. Chinga-Carrasco, Wide range humidity sensors printed on biocomposite fi lms of cellulose nano fi bril and poly (ethylene glycol), J. Appl. Polym. Sci. 47920 (2019) 1–10. doi:10.1002/app.47920.

[14] G. Chinga-Carrasco, N. Ehman, J. Pettersson, M. Vallejos, M. Brodin, F. Felissia, J.

Håkansson, M.C. Area, Pulping and Pretreatment Affect the Characteristics of Bagasse Inks for Three-dimensional Printing, ACS Sustain. Chem. Eng. 6 (2018). doi:10.1021/acssuschemeng.7b04440.

[15] J.M. Lagaron, A. Lopez-Rubio, Nanotechnology for bioplastics : opportunities , challenges and strategies, Trends Food Sci. Technol. 22 (2011) 611–617. doi:10.1016/j.tifs.2011.01.007.

[16] M. Wang, I. V Anoshkin, A.G. Nasibulin, J.T. Korhonen, J. Seitsonen, J. Pere, E.I. Kauppinen, R.H.A. Ras, O. Ikkala, Modifying native nanocellulose aerogels with carbon nanotubes for mechanoresponsive conductivity and pressure sensing, Adv. Mater. 25 (2013) 2428–2432. doi:10.1002/adma.201300256.

[17] F. Liebner, E. Haimer, M. Wendland, M. Neouze, K. Schlufter, P. Miethe, T. Heinze, A. Potthast, T. Rosenau, Aerogels from unaltered bacterial cellulose : Application of scCO2 drying for the preparation of shaped , ultra-lightweight cellulosic aerogels, Macromol. Biosci. 10 (2010) 349–352. doi:10.1002/mabi.200900371.

[18] I. Besbes, S. Alila, S. Boufi, Nanofibrillated cellulose from TEMPO-oxidized eucalyptus fibres: effect of the carboxyl content, Carbohydr. Polym. 84 (2011) 975–983. doi:10.1016/j.carbpol.2010.12.052.

[19] G. Chinga-Carrasco, Optical methods for the quantification of the fibrillation degree of bleached MFC materials, Micron. 48 (2013) 42–48. doi:10.1016/j.micron.2013.02.005.

[20] O. Laitinen, Utilisation of tube flow fractionation in fibre and particle analysis, University of Oulu, 2011.

[21] A. Tanaka, T. Hjelt, A. Sneck, A. Korpela, Fractionation of Nanocellulose by Foam Filter, Sep. Sci. Technol. 47 (2012) 1771–1776. doi:10.1080/01496395.2012.661825.

[22] A. Tanaka, V. Seppanen, J. Houni, Nanocellulose characterization with mechanical fractionation, Nord. Pulp Pap. Res. J. 27 (2012) 689–694. doi:10.3183/NPPRJ-2012-27-04-p689-694.

[23] J. Gamelas, J. Pedrosa, A. Lourenço, P. Mutjé, I. González, G. Chinga-Carrasco, G. Singh, P.J. Ferreira, A. Lourenco, P. Mutjé, I. Gonzáles, G. Chinga-Carrasco, S. Gurvinder, P.J. Ferreira, On the morphology of cellulose nanofibrils obtained by TEMPO-mediated

oxidation and mechanical treatment, Micron. 72 (2015) 28–33. doi:10.1016/j.micron.2015.02.003.

[24] G. Albornoz, A. Andrade, M. Pereira, Study of the relationship between intrinsic viscosit and aspect ratio of cellulose nanofibers suspensions, in: 51° Pulp Pap. Int. Congr. X Iberoam. Congr. Pulp Pap., São Paulo, 2018: pp. 23–25.

[25] T. Moberg, K. Sahlin, K. Yao, S. Geng, G. Westman, Q. Zhou, K. Oksman, M. Rigdahl, Rheological properties of nanocellulose suspensions: effects of fibril/particle dimensions and surface characteristics, Cellulose. 24 (2017) 2499–2510. doi:10.1007/s10570-017-1283-0.

[26] S. Iwamoto, A. Nakagaito, H. Yano, Nano-fibrillation of pulp fibers for the processing of transparent nanocomposites, App. Phys. A. 89 (2007) 461–466. doi:10.1007/s00339-007-4175-6.

[27] E. Espinosa, Q. Tarrés, M. Delgado-Aguilar, I. Gonzáles, P. Mutjé, A. Rodríguez, Suitability of wheat straw semichemical pulp for the fabrication of lignocellulosic nanofibres and their application to papermaking slurries, Cellulose. 23 (2015) 837–852. doi:10.1007/s10570-015-0807-8.

[28] N. Ehman, Q. Tarrés, M. Delgado-Aguilar, M. Vallejos, F. Felissia, M.C. Area, P. Mutjé, From pine sawdust to cellulose nanofibers, Cellul. Chem. Technol. 50 (2016) 361–367. http://www.cellulosechemtechnol.ro/pdf/CCT3-4(2016)/p.361-367.pdf.

[29] A. Isogai, T. Saito, H. Fukuzumi, TEMPO-oxidized cellulose nanofibers, Nanoscale. 3 (2011) 71–85. doi:10.1039/c0nr00583e.

[30] M. Vallejos, F. Felissia, M.C. Area, N. Ehman, Q. Tarrés, P. Mutjé, Nanofibrillated cellulose (CNF) from eucalyptus sawdust as a dry strength agent of unrefined eucalyptus handsheets, Carbohydr. Polym. 139 (2016) 99–105. doi:10.1016/j.carbpol.2015.12.004.

[31] Q. Tarrés, N. Ehman, M. Vallejos, M.C. Area, M. Delgado-Aguilar, P. Mutjé, Lignocellulosic nanofibers from triticale straw : The influence of hemicelluloses and lignin in their production and properties, Carbohydr. Polym. 163 (2017) 20–27.

[32] A. Balea, N. Merayo, E.D. La Fuente, C. Negro, Á. Blanco, Assessing the influence of refining , bleaching and TEMPO-mediated oxidation on the production of more sustainable cellulose nanofibers and their application as paper additives, Ind. Crop. Prod. 97 (2017)

374–387. doi:10.1016/j.indcrop.2016.12.050.

[33] S.R. Djafari Petroudy, A. Ghasemian, H. Resalati, K. Syverud, G. Chinga-Carrasco, The effect of xylan on the fibrillation efficiency of DED bleached soda bagasse pulp and on nanopaper characteristics, Cellulose. 22 (2015) 385–395. doi:10.1007/s10570-014-0504-z.

[34] G. Ayissi Eyebe, B. Bideau, N. Boubekeur, É. Loranger, F. Domingue, Environmentally-friendly cellulose nanofibre sheets for humidity sensing in microwave frequencies, Sensors Actuators, B Chem. 245 (2017) 484–492. doi:10.1016/j.snb.2017.01.130.

[35] R. Sánchez, E. Espinosa, J. Domínguez-robles, J. Mauricio, A. Rodríguez, International Journal of Biological Macromolecules Isolation and characterization of lignocellulose nanofibers from different wheat straw pulps, Int. J. Biol. Macromol. 92 (2016) 1025–1033. doi:10.1016/j.ijbiomac.2016.08.019.

[36] T. Saito, A. Isogai, TEMPO-mediated oxidation of native cellulose . The effect of oxidation conditions on chemical and crystal structures of the water-insoluble fractions, Biomacromolecules. 5 (2004) 1983–1989. doi:10.1021/bm0497769.

[37] A. Dufresne, Cellulose microfibrils from potato tuber cells : Processing and characterization of starch – cellulose microfibril composites, J. Appl. Polym. Sci. 76 (1999) 2080–2092. doi:10.1002/(SICI)1097-4628(20000628)76:143.0.CO;2-U.

[38] S. Lee, S. Chun, I. Kang, J. Park, Preparation of cellulose nanofibrils by high-pressure homogenizer and cellulose-based composite films, J. Ind. Eng. Chem. 15 (2009) 50–55. doi:10.1016/j.jiec.2008.07.008.

[39] I. Siró, D. Plackett, Microfibrillated cellulose and new nanocomposite materials: a review, Cellulose. 17 (2010) 459–494. doi:10.1007/s10570-010-9405-y.

[40] K. Uetani, H. Yano, Nanofibrillation of wood pulp using a high-speed blender, Biomacromolecules. 12 (2011) 348–353. doi:10.1021/bm101103p.

[41] A. Balea, J. Sanchez-salvador, M.C. Monte, N. Merayo, C. Negro, A. Blanco, In situ production and application of cellulose nanofibers to improve recycled paper production, (2019) 1–13.

[42] M. Delgado-Aguilar, I. González, Q. Tarrés, M.À. Pèlach, M. Alcalà, P. Mutjé, The key role of lignin in the production of low-cost lignocellulosic nanofibres for papermaking

applications, Ind. Crop. Prod. 86 (2016) 295–300. doi:10.1016/j.indcrop.2016.04.010.

[43] T. Pääkkönen, K. Dimic-Misic, H. Orelma, R. Pönni, T. Vuorinen, T. Maloney, Effect of xylan in hardwood pulp on the reaction rate of TEMPO-mediated oxidation and the rheology of the final nanofibrillated cellulose gel, Cellulose. 23 (2016) 277–293. doi:10.1007/s10570-015-0824-7.

[44] N. Ehman, G. Rodriguez Rivero, M.C. Area, F. Felissia, Dissolving pulps by oxidation of the Cellulosic fraction of lignocellulosic waste, Cellul. Chem. Technol. 51 (2017). http://www.cellulosechemtechnol.ro/downloadfirstonline.php?file=8113.

[45] C. Imlauer, J. Kruyeniski, M.C. Area, F. Felissia, Fraccionamiento a la Soda-AQ de aserrín de pino para la biorefinería forestal, in: VIII CIADICYP VIIIIberoAmerican Congr. Pulp Pap. Res., Medellín, 2014: pp. 26–28.

[46] A. Sluiter, B. Hames, R. Ruiz, C. Scarlata, Determination of structural carbohydrates and lignin in biomass determination of structural carbohydrates and lignin in biomass, 2011. https://www.nrel.gov/docs/gen/fy13/42618.pdf (accessed March 30, 2015).

[47] P. Mocchiutti, M. Galván, S. Peresin, C. Schnell, M. Zanutiini, Complexes of xylan and synthetic polyelectrolytes. Characterization and adsorption onto high quality unbleached fibers, Carbohydr. Polym. 116 (2014) 131–139.

[48] G. Chinga-Carrasco, N. Averianova, O. Kondalenko, M. Garaeva, V. Petrov, B. Leinsvang, T. Karlsen, The effect of residual fibres on the micro-topography of cellulose nanopaper, Micron. 56 (2014) 80–84. doi:10.1016/j.micron.2013.09.002.

[49] L. Segal, A. Greely, A. Martin, C. Conrad, Empirical Method for Estimating the Degree of Crystallinity of Native Cellulose Using the X-Ray Diffractometer, Text. Res. J. 29 (1959) 786–794.

[50] H. Sixta, Handbook of Pulp Volume I, Weinheim, 2006.

[51] A. Balea, N. Merayo, E. Fuente, M. Delgado-Aguilar, P. Mutjé, A. Blanco, N. Carlos, Valorization of Corn Stalk by the Production of Cellulose Nanofibers to Improve Recycled Paper Properties, BioResources. 11 (2016) 3416–3431. doi:10.15376/biores.11.2.3416-3431.

[52] M. Hubbe, O. Rojas, L. Lucia, M. Sain, Cellulosic nanocomposites: a review, BioResources. 3 (2008) 929–980.

http://ojs.cnr.ncsu.edu/index.php/BioRes/article/view/BioRes_03_3_0929_Hubbe_RLS_Cellulosic_Nanocomposites_Rev (accessed March 30, 2015).

[53] R. Tanaka, T. Saito, D. Ishii, A. Isogai, Determination of nanocellulose fibril length by shear viscosity measurement, Cellulose. 21 (2014) 1581–1589. doi:10.1007/s10570-014-0196-4.

[54] M. Delgado Aguilar, Nanotecnología en el sector papelero: mejoras en calidad y permanencia de las fibras de alto rendimiento y secundarias en una economía circular mediante el uso de nanofibras y el refino enzimático, 2015. http://dugi-doc.udg.edu/handle/10256/11737.

[55] E. Sánchez-Safont, A. Aldureid, M.J. Lagarón, J. Gámez-Pérez, L. Cabedo, Biocomposites of di ff erent lignocellulosic wastes for sustainable food packaging applications, Compos. Part B. 145 (2018) 215–225. doi:10.1016/j.compositesb.2018.03.037.

Table 1. Summary of the treatments applied on raw materials

Pulp	Raw Material	Pulping Process	Sample
A	Eucalyptus sawdust	Soda TCF bleached (O-Op sequence)	LCNF1
B	Sugarcane bagasse	Soda/AQ + O_2	LCNF2
C	Pine chips	Commercial ECF bleached Kraft	LCNF3
D	Pine sawdust	Soda/Ethanol TCF Bleached (O-O-Z sequence)	LCNF4
E		Soda/Ethanol, Unbleached	LCNF5
F		Soda/Oxygen, Unbleached	LCNF6
G		Soda/Oxygen, Unbleached	LCNF7

O: Oxygen stage, Op: Oxygen stage reinforced with peroxide, Z: ozone stage

Table 2. Characterization of the initial pulps

Pulp	Chemical composition (% odp)						Intrinsic viscosity (mL/g)	Carboxylate content (µmol/g)
	Glu	*Lig*	Hemicelluloses					
			Xyl	*Man*	*Ara*	*Gal*		
A	73.9	0.8	18.9	0.0	0.0	0.0	756	132.8
B	67.1	1.9	23.0	3.1	0.4	1.8	960	73.7
C	81.2	0.05	7.3	9.3	0.4	0.4	711	15.3
D	75.2	3.8	7.0	7.7	0.4	0.0	442	104.1
E	76.1	3.7	8.4	7.7	0.3	0.0	767	148.5
F	70.7	14.5	4.7	8.0	0.3	0.3	570	208.7
G	82.7	4.6	4.2	7.2	0.3	0.0	348	183.5

odp: oven-dry pulp. Xyl: xylans. Man: mannans. Gal: galactans. Ara: arabinans.

Table 3. LCNF characterization

Pulp	Sample	Oxidation time (min)	Carboxylate groups (μmol/g)	Viscosity (Pa.s)	Nanofibrillation Yield (%)	Transmittance (%)	Turbidity (NTU)	Cationic demand (μeq/g)
A	LCNF1	150	908 ± 11	12.1	--	68.9	39.1	1012
B	LCNF2	105	817 ± 19	37.4	56.2	64.0	68.7	900
C	LCNF3	120	1005 ± 16	69.5	62.4	79.6	37.1	1231
D	LCNF4	90	866 ± 8	11.0	63.0	75.8	53.5	1685
E	LCNF5	90	787 ± 1	40.2	57.1	64.0	69.7	1501
F	LCNF6	60	705 ± 9	9.8	55.1	59.6	86.9	899
G	LCNF7	90	638 ± 4	9.7	59.6	67.0	61.6	908

Graphical abstract

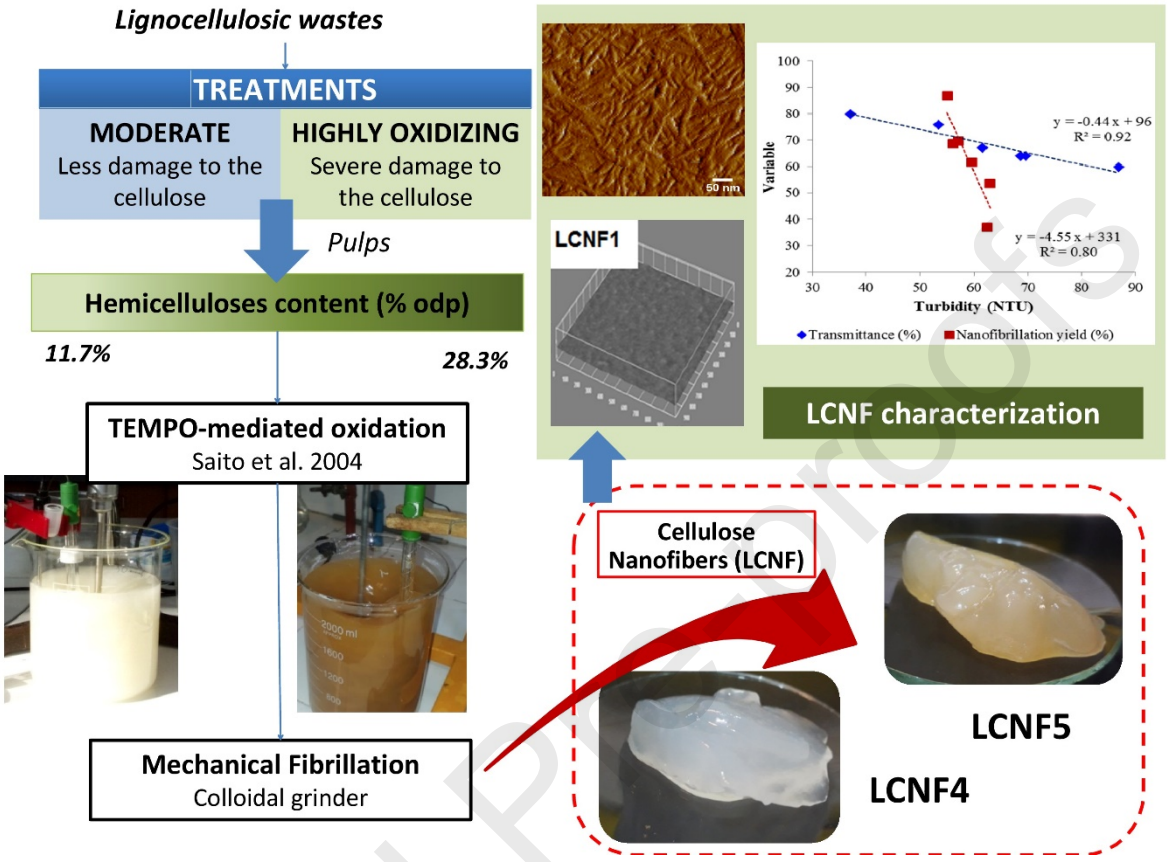

Highlights (for review)

- ✓ Influence of the initial characteristics of pulps on production process and final properties of lignocellulosic nanofibers
- ✓ Relationships between methods to measure final properties of lignocellulosic nanofibers
- ✓ Component analysis (PCA) to evaluate variables that allow highly or lowly fibrillated LCNF

Influence of initial chemical composition and characteristics of pulps on the production and properties of lignocellulosic nanofibers

Ehman N.V.[a*], Lourenço A.F.[b], McDonagh B.H.[c], Vallejos, M.E.[a], Felissia F.E.[a], Ferreira P.J.T.[b], Chinga-Carrasco G.[c], Area M.C.[a]

Figure 1.

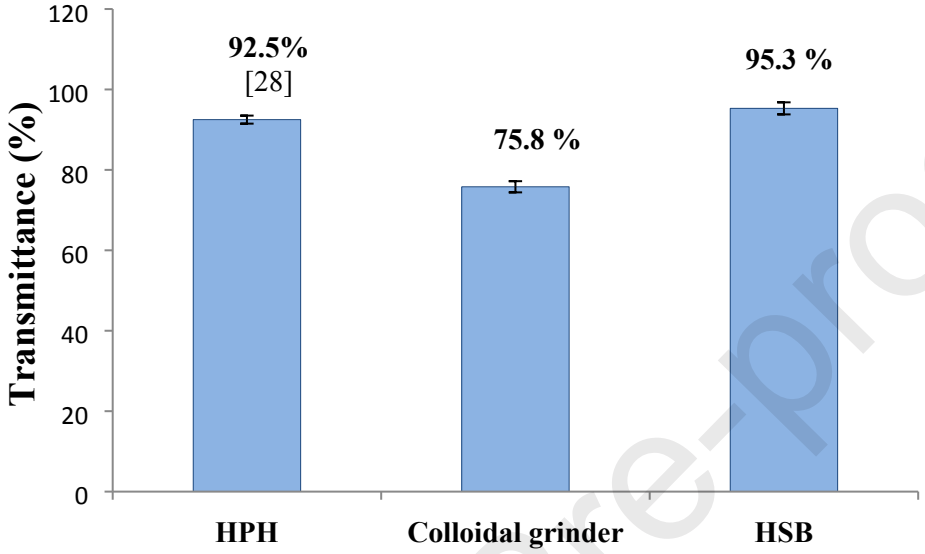

Influence of initial chemical composition and characteristics of pulps on the production and properties of lignocellulosic nanofibers

Ehman N.V.[a*], Lourenço A.F.[b], McDonagh B.H.[c], Vallejos, M.E.[a], Felissia F.E.[a], Ferreira P.J.T.[b], Chinga-Carrasco G.[c], Area M.C.[a]

Figure 2.

Laser profilometry Roughness (µm)				
0.38 ± 0.01	1.39 ± 0.15	0.97 ± 0.09	2.45 ± 0.09	1.49 ± 0.08

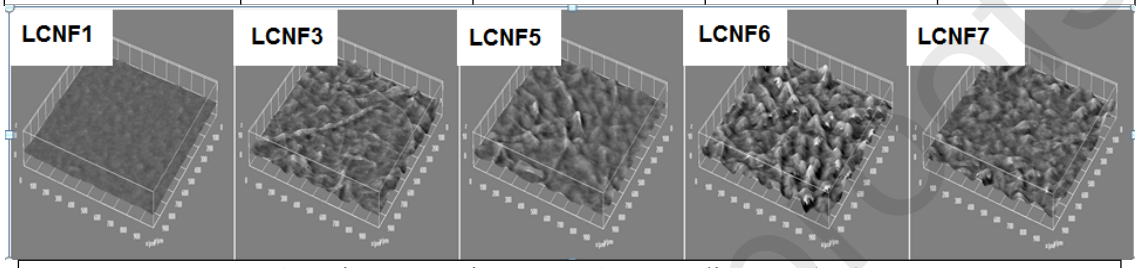

Atomic Force Microscopy Average diameter (nm)				
11.8 ± 5.0	11.7 ± 4.0	8.6 ± 2.7	8.9 ± 1.1	11.0 ± 1.6

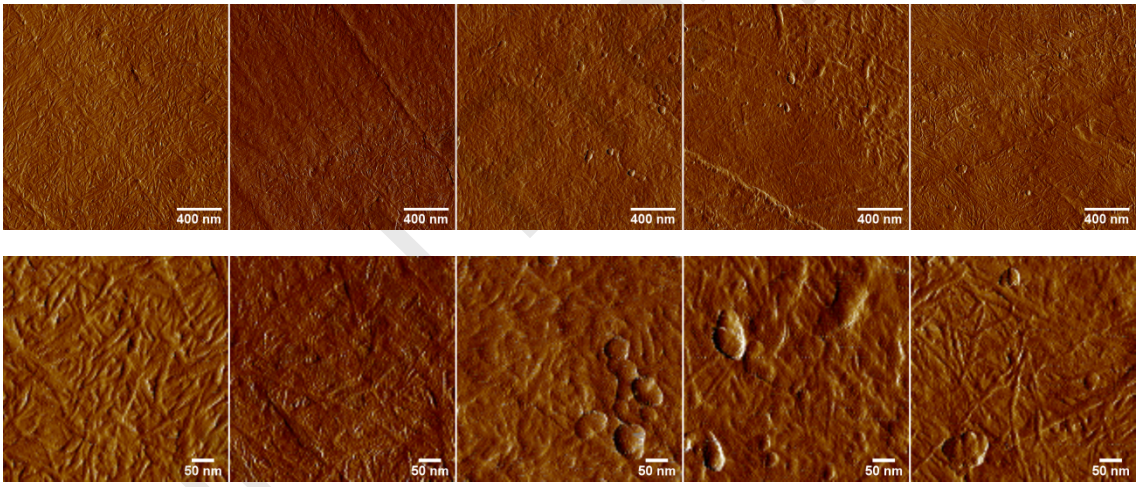

Influence of initial chemical composition and characteristics of pulps on the production and properties of lignocellulosic nanofibers

Ehman N.V.[a*], Lourenço A.F.[b], McDonagh B.H.[c], Vallejos, M.E.[a], Felissia F.E.[a], Ferreira P.J.T.[b], Chinga-Carrasco G.[c], Area M.C.[a]

Figure 3.

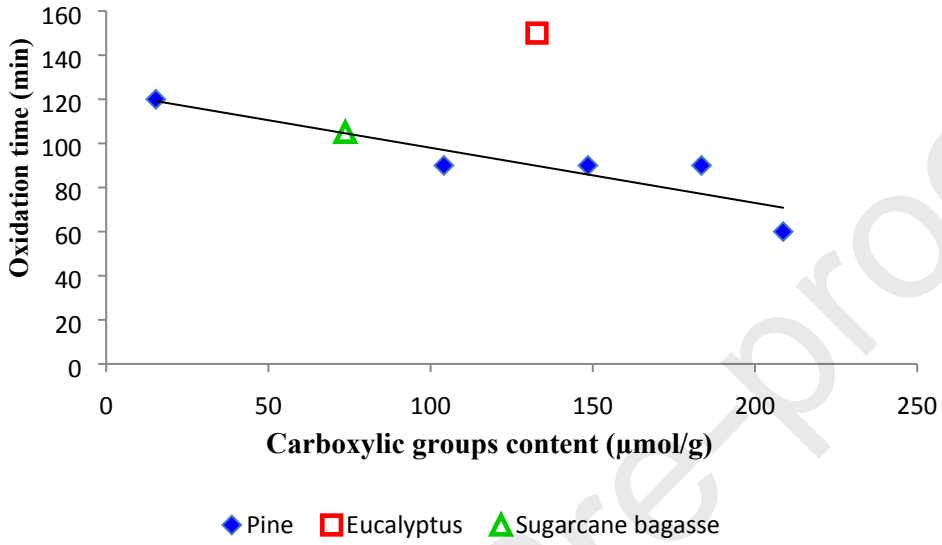

Influence of initial chemical composition and characteristics of pulps on the production and properties of lignocellulosic nanofibers

Ehman N.V.[a*], Lourenço A.F.[b], McDonagh B.H.[c], Vallejos, M.E.[a], Felissia F.E.[a], Ferreira P.J.T.[b], Chinga-Carrasco G.[c], Area M.C.[a]

Figure 4.

(a)

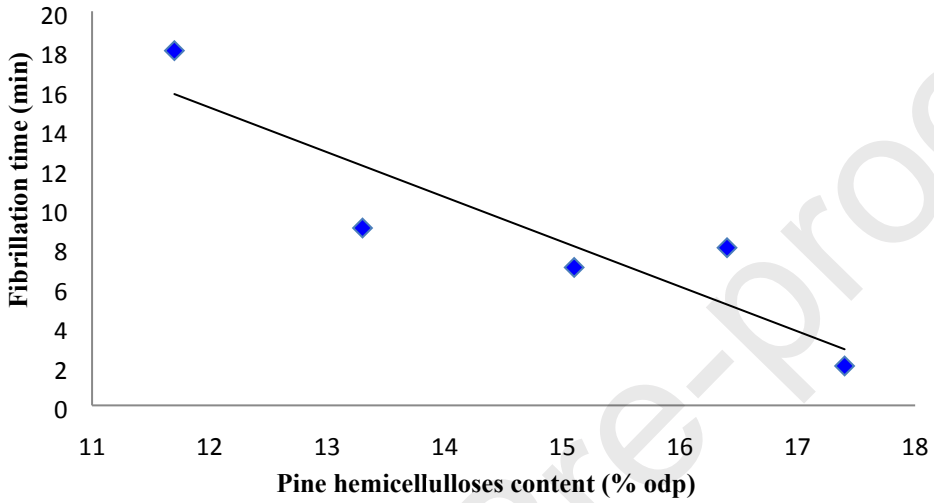

(b)

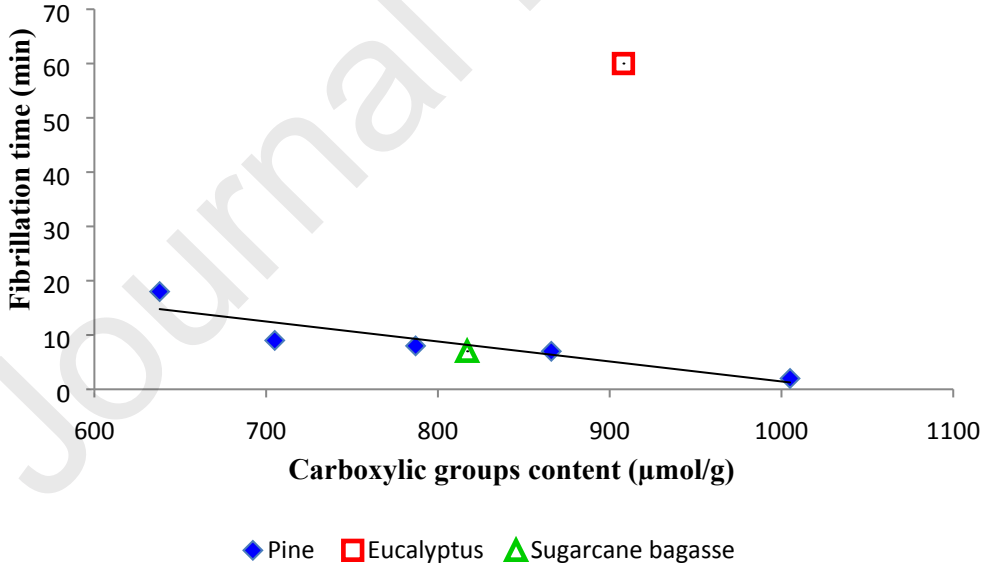

Influence of initial chemical composition and characteristics of pulps on the production and properties of lignocellulosic nanofibers

Ehman N.V.[a*], Lourenço A.F.[b], McDonagh B.H.[c], Vallejos, M.E.[a], Felissia F.E.[a], Ferreira P.J.T.[b], Chinga-Carrasco G.[c], Area M.C.[a]

Figure 5.

(a)

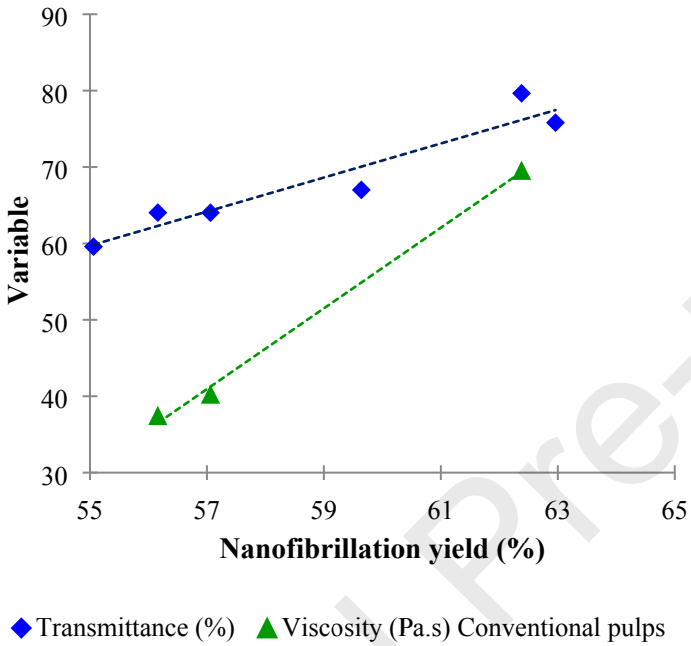

(b)

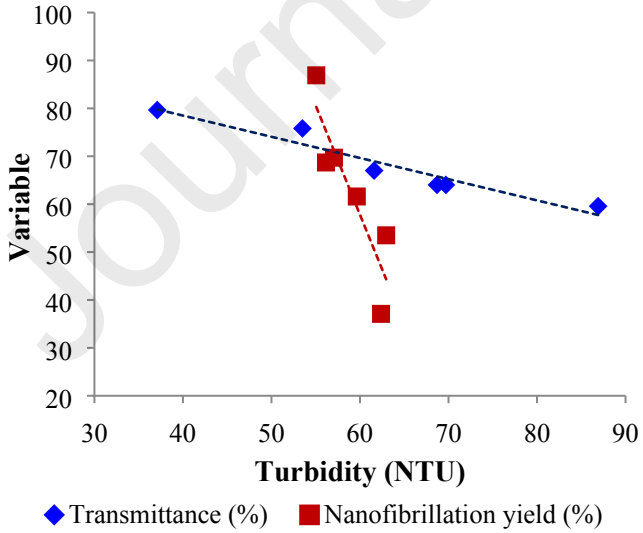

Influence of initial chemical composition and characteristics of pulps on the production and properties of lignocellulosic nanofibers

Ehman N.V.[a*], Lourenço A.F.[b], McDonagh B.H.[c], Vallejos, M.E.[a], Felissia F.E.[a], Ferreira P.J.T.[b], Chinga-Carrasco G.[c], Area M.C.[a]

Figure 6.

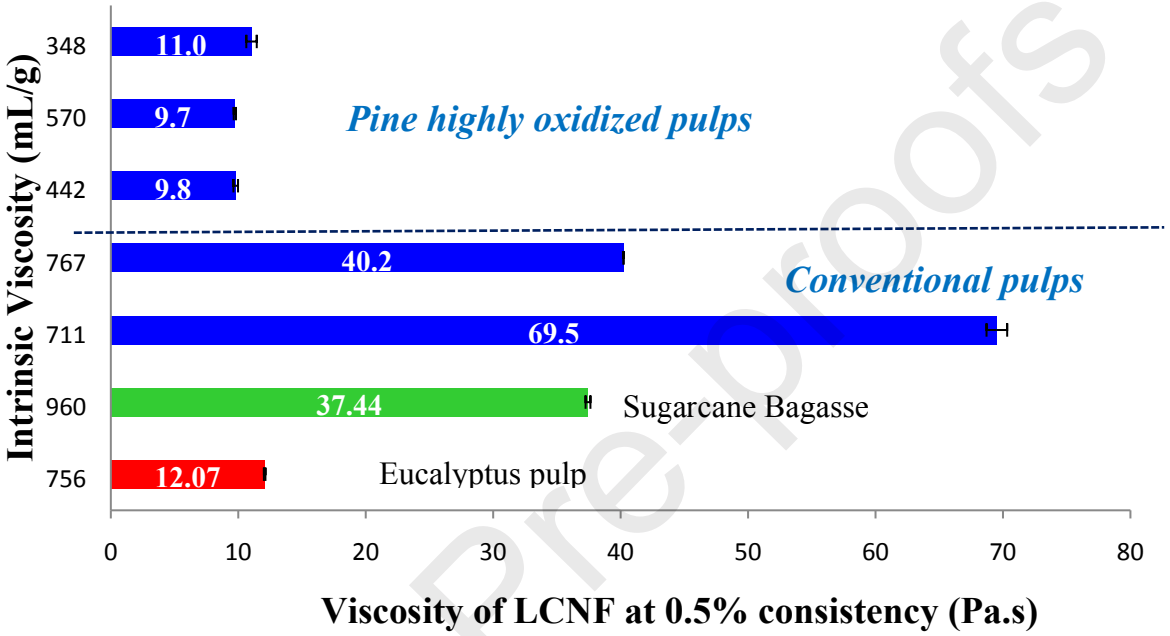

Influence of initial chemical composition and characteristics of pulps on the production and properties of lignocellulosic nanofibers

Ehman N.V.[a*], Lourenço A.F.[b], McDonagh B.H.[c], Vallejos, M.E.[a], Felissia F.E.[a], Ferreira P.J.T.[b], Chinga-Carrasco G.[c], Area M.C.[a]

Figure 7.

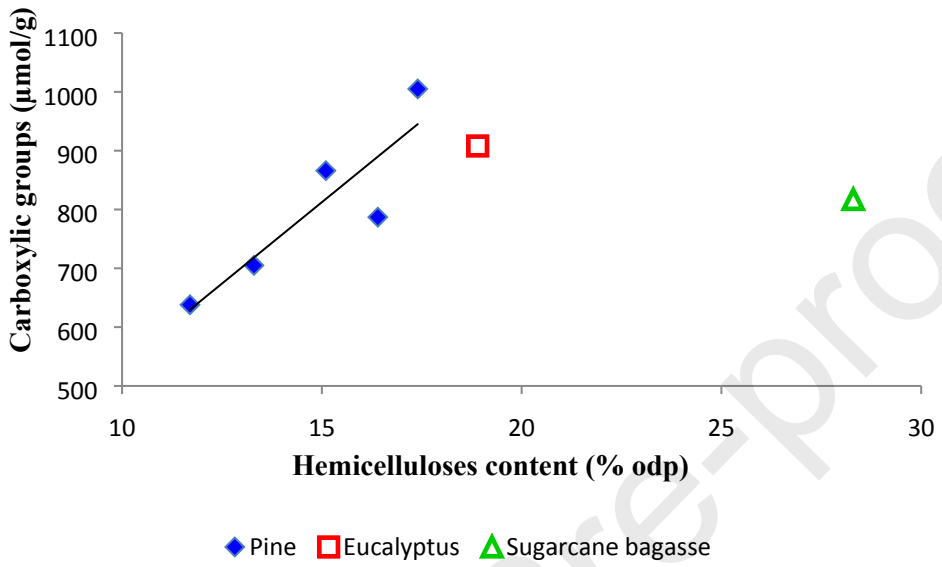

Caption of figures

Figure 1. Comparison between types of equipment for mechanical fibrillation of soda-ethanol TCF bleached pine sawdust pulp (D) and soda/AQ-O-Z pine sawdust pulp (previous study [27]).

Figure 2. Multi-scale assessment of LCNF films. Upper row: Laser profilometry. Middle row: AFM images (2 μm x 2 μm). Lower row: AFM images of selected areas (500 nm x 500 nm).

Figure 3. Relationship between TEMPO mediated oxidation time with carboxylate groups content in initial pulps

Figure 4. Relationship between mechanical fibrillation time and: (a) hemicelluloses content of pine pulps; (b) carboxylic groups of TEMPO oxidized pulps.

Figure 5. Relationships between different properties and the degree of fibrillation: a. Nanofibrillation yield vs. viscosity and transmittance, b. Transmittance and nanofibrillation yield vs. turbidity.

Figure 6. Comparison between viscosity of LCNF (at 0.5% consistency and 0.6 rpm) from conventional and highly oxidized pine pulps, conventional eucalyptus pulp and conventional sugarcane bagasse pulp.

Figure 7: Relationship between hemicelluloses content in pulps and carboxylate groups in LCNF.